ELSEVIER

Geomorphology 35 (2000) 193–217

GEOMORPHOLOGY

www.elsevier.nl/locate/geomorph

Bank and near-bank processes in an incised channel

Andrew Simon [a,*], Andrea Curini [a], Stephen E. Darby [b], Eddy J. Langendoen [a]

[a] *USDA, Agricultural Research Service, National Sedimentation Laboratory, 598 McElroy Drive, P.O. Box 1157, Oxford, MS 38655, USA*
[b] *Department of Geography, University of Southampton, Southampton, UK*

Received 4 February 1999; received in revised form 11 June 1999; accepted 13 June 1999

Abstract

Gravitational forces acting on in situ bank material act in concert with hydraulic forces at the bank toe to determine rates of bank erosion. The interaction of these forces control streambank mechanics. Hydraulic forces exerted by flowing water on in situ bank-toe material and failed cohesive material at the bank toe are often sufficient to entrain materials at relatively frequent flows and to maintain steep lower-bank profiles. Seepage forces exerted on in situ bank material by groundwater, downward infiltration of rainwater and lateral seepage of streamflow into and out of the bank are critical in determining bank strength. Data from a study site on Goodwin Creek, MS, USA clearly show the temporal variability of seepage forces and the lag time inherent in reductions in shear strength due to losses of matric suction and generation of positive pore-water pressures. Negative pore-water pressures (matric suction) have also been shown to increase the resistance of failed cohesive blocks to entrainment by fluid shear. A stable bank can be transformed into an unstable bank during periods of prolonged rainfall through:

1. increase in soil bulk unit (specific) weight,
2. decrease or complete loss of matric suction, and, therefore, apparent cohesion,
3. generation of positive pore-water pressures, and, therefore, reduction or loss of frictional strength,
4. entrainment of in situ and failed material at the bank toe, and
5. loss of confining pressure during recession of stormflow hydrographs.

Relatively small frequent flows during the winter have the ability to erode failed bank materials, maintain oversteepened, unstable bank surfaces and promote prolonged periods of bank retreat, channel migration and high yields of fine-grained sediment. Confining pressures provided by stormflow are not as significant in maintaining bank stability as the counteracting force of fluid shear on the bank toe, which steepens the bank. For example, more than 2 m of bank retreat occurred during the study period at the research site on Goodwin Creek, northern Mississippi. The loss of matric suction (negative pore pressures) due to infiltrating precipitation has been found to be as significant as the development of excess pore pressures in contributing to mass bank instability. Apparent cohesion, friction angle, soil bulk unit weight and moisture content were

* Corresponding author. Tel.: +1-601-232-2918; fax: +1-601-232-2915.
E-mail address: simon@sedlab.olemiss.edu (A. Simon).

0169-555X/00/$ - see front matter
PII: S0169-555X(00)00036-2

measured in situ. Matric suction was measured continuously, in situ with a series of five pressure-transducer tensiometers. A bank-failure algorithm, which combines the Mohr–Coulomb approach, for saturated conditions and the Fredlund modification for unsaturated conditions was developed for layered cohesive streambanks. The resulting equation has been used successfully to investigate the role of matric suction, positive pore-water pressures and confining pressure for layered streambanks composed of cohesive materials.

Keywords: pore-water pressure; bank erosion; bank-toe material; bank-stability model

1. Introduction

The adjustment of channel width by mass-wasting and related processes represents an important mechanism of channel response and energy dissipation in incised alluvial streams. In the loess area of the Midwest United States, for example, bank material contributes as much as 80% of the total sediment eroded from incised channels (Simon et al., 1996). In unstable streams, rates of width adjustment by mass-wasting processes can occur over several orders of magnitude: 1.5 m/year in the Obion–Forked Deer River System, West TN (Simon, 1989a); 14 m/year in the Cimarron River, KS (Schumm and Lichty, 1963); about 50 m/year in the Gila River, AZ; and more than 100 m/year in some reaches of the Toutle River System, WA (Simon, 1992). The Brahmaputra River commonly adjusts its width from 50–1100 m/year (Thorne, 1999, personal communication). The range of rates reflects a diversity of channel-disturbance characteristics, environmental settings and boundary materials.

Conceptual models of bank retreat and the delivery of bank sediments to the flow emphasize the importance of interactions between hydraulic forces acting at the bed and bank toe, and gravitational forces acting on in situ bank (Carson and Kirkby, 1972; Thorne, 1982; Simon et al., 1991). Failure occurs when erosion of the bank toe and the channel bed adjacent to the bank have increased the height and angle of the bank to the point that gravitational forces exceed the shear strength of the bank material. Failed bank materials may be delivered directly to the flow and deposited as bed material, dispersed as wash load, deposited along the toe of the bank as intact blocks, or as smaller dispersed aggregates (Simon et al., 1991). If deposited at the bank toe, failed bank material may temporarily increase bank stability by buttressing the bank and protecting in situ bank material from attack and entrainment by the flow. The properties of the failed bank material, in tandem with the hydraulic forces acting at the bank toe, control the residence time of failed bank material (Thorne, 1978).

Recently, attempts have been made to apply mass-wasting analyses of in situ bank materials (e.g., Little, 1982; Osman and Thorne, 1988; Lohnes, 1991; Simon et al., 1991; Casagli, 1994; Darby, 1994) in conjunction with hydraulic and sediment transport models to simulate interactions between bed (hydraulic) and bank (gravitational) processes and hence channel adjustment and evolution (Simon et al., 1991; Darby, 1994; Simon and Darby, 1997a). However, these attempts are limited by a lack of understanding of the way in which hydraulic and gravitational processes interact to control long-term rates of bank retreat, channel migration and the development of equilibrium channel morphology.

2. Purpose

This paper addresses many of the fundamental issues related to the interaction of fluvial and geotechnical processes affecting streambanks and the near-bank zone. In particular, the research described here evaluates specific forces and processes controlling bank failures and channel widening in incised channels. These include:

1. the role of negative pore pressures (matric suction) in the unsaturated zone in increasing bank strength, contrasted with the role of positive pore-water pressures in reducing bank strength;

2. the role of hydraulic forces causing bank erosion and steepening of toe profiles, contrasted with hydrostatic forces providing support for the bank through confining pressure;
3. the effects of variability of moisture content with time on other geotechnical properties; and
4. development of a bank-stability algorithm for layered cohesive streambanks, which encompasses positive and negative pore-water pressures as well as confining pressures, and the vertical and temporal variability of soil properties.

3. The nature of streambank failures

Bank failures can be characterized by the shape of the failure surface (planar and rotational) or by the mode of failure. Rotational failures, although more damaging in terms of loss of land and generally less common along streambanks than other failure types, occur along the highest banks (Simon, 1989a; Thorne, 1990) because shear stress increases quicker with depth than does shear strength (Terzaghi and Peck, 1948). As incised channels evolve with time, planar failures often occur earlier in the adjustment sequence than do rotational failures when banks are lower (Simon, 1989b) and can occur along any critical failure plane, irrespective of whether that plane passes through the toe of the bank. Slab failures (planar) generally result from fluvial undercutting and/or the development of a near-vertical tension crack in the upper part of the bank (Lohnes and Handy, 1968; Thorne et al., 1981). Pop-out failures can occur at the base of the bank (Bradford and Piest, 1980) or in areas of contrasting permeabilities (Simon and Darby, 1997b) from the generation of pore-water pressures that exceed the tensile and shear strength of the bank materials.

Bank failures have been most commonly reported during the recessional period of stormflow and often can be represented analytically, as a saturated rapid-drawdown condition (Simon and Hupp, 1987; Thorne, 1990). In terms of broader temporal and spatial scales, the occurrence of bank failures generally indicates channel instability of an unspecified magnitude and spatial extent and can signify instability of channel pattern.

4. Forces controlling bank failures in incised alluvial channels

To better understand the complex interaction of hydraulic and geotechnical forces and processes affecting streambank mechanics, it is helpful to conceptualize these interactions in terms of typical driving forces and resisting forces during the course of incised channel evolution. Channel evolution refers to systematic temporal and spatial adjustments to morphology.

The equilibrium channel represents the initial predisturbed stage (I) of channel evolution and the disrupted channel as an instantaneous condition (stage II). Rapid channel degradation of the channel bed ensues as the channel begins to adjust (stage III). Degradation flattens channel gradients and consequently reduces the available stream power for given discharges with time. Concurrently, bank heights are increased and bank angles are often steepened by fluvial undercutting and by pore-pressure induced bank failures near the base of the bank. Thus, the degradation stage (III) is directly related to destabilization of the channel banks and leads to channel widening by mass-wasting processes (stage IV) once bank heights and angles exceed the critical shear strength conditions of the bank material. The aggradation stage (V) becomes the dominant trend in previously degraded downstream sites as degradation migrates further upstream because the flatter gradient at the degraded site cannot transport the increased sediment loads emanating from degrading reaches upstream. This secondary aggradation occurs at rates roughly 60–75% less than the associated degradation rate (Simon, 1992). These milder aggradation rates indicate that bed-level recovery will not be complete and that attainment of a new dynamic equilibrium (stage VI) will take place through further (1) bank widening and the consequent flattening of bank slopes, (2) the establishment and proliferation of riparian vegetation that adds roughness elements, enhances bank accretion and reduces the stream power for given discharges, and (3) further gradient reduction by meander extension and elongation.

4.1. Geotechnical forces

If we initially envision a channel deepened by bed degradation in which the streambanks have not yet

begun to fail, the gravitational force acting on the bank cannot overcome the resistance (shear strength) of the in situ bank material. For the simple case of a planar failure of unit width and length, bank resistance can be represented by a revised Coulomb equation:

$$S_r = c' + (\sigma - \mu)\tan\phi' \quad (1)$$

where S_r = shear strength; c' = effective cohesion (kPa); σ = normal stress (kPa); μ = pore-water pressure (kPa) and ϕ' = effective friction angle (°). The normal stress is given by:

$$\sigma = W\cos\beta \quad (1a)$$

where W = weight of the failure block and β = angle of the failure plane. The driving (gravitational) force for this example is given by (S_d):

$$S_d = W\sin\beta \quad (2)$$

A factor of safety (F_s) is expressed then as the ratio between the resisting forces (Eq. (1)) and the driving, gravitational forces (Eq. (2)). A value of unity indicates the critical case and imminent failure.

4.2. Effect of pore-water pressures

The effect of excess pore-water pressures in reducing bank strength under saturated conditions has long been identified as an important contributor to streambank and hillslope instability. Streambank failures are often observed to occur on the recessional limb of storm hydrographs. This has been attributed to rapid-drawdown conditions in the channel banks, where positive pore-water pressures are not counteracted by confining pressure afforded by the water in the channel. Recently, it has been found that positive or excess pore-water pressures may not be required to establish a rapid-drawdown condition that results in mass failure. In fact, field data indicate that the loss of negative pore-water pressures, or matric suction, can play an important role in initiating bank instabilities following periods of rainfall (Casagli et al., 1997, 1999; Curini, 1998; Simon and Curini, 1998).

Incised streams generally have high banks where the phreatic surface is usually deep relative to the total bank height during low and even moderate river stages. Above the water table, the soil has a degree of saturation less than 100% and negative pore-water pressures develop. Thus, a large proportion of the streambanks of an incised channel can be characterized as unsaturated. For these circumstances, where a good portion of the failure surface might pass through unsaturated soil, slope stability analyses incorporating unsaturated shear strength parameters are required to predict stability accurately.

In the part of the streambank above the "normal" level of the groundwater table, bank materials are unsaturated, pores are filled with water and air, and pore-water pressure is negative. The difference ($\mu_a - \mu_w$) between the air pressure (μ_a) and the water pressure in the pores (μ_w) represents the matric suction (ψ). The increase in shear strength due to an increase in matric suction is described by the angle ϕ^b. Incorporating this effect into the standard Mohr–Coulomb equation produces (Fredlund et al., 1978):

$$S_r = c' + (\sigma - \mu_a)\tan\phi' + (\mu_a - \mu_w)\tan\phi^b \quad (3)$$

where $(\sigma - \mu_a)$ = net normal stress on the failure plane at failure; μ_w = pore-water pressure on the failure plane at failure. The value of ϕ^b is generally between 10° and 20°, and increases with the degree of saturation. It attains a maximum value of ϕ' under saturated conditions (Fredlund and Rahardjo, 1993). The effects of matric suction on shear strength is reflected in the apparent or total cohesion (c_a) term although this does not signify that matric suction is a form of cohesion (Fredlund and Rahardjo, 1993):

$$c_a = c' + (\mu_a - \mu_w)\tan\phi^b = c' + \psi\tan\phi^b \quad (4)$$

As can be seen from Eq. (4), negative pore-water pressures (positive matric suction; ψ) in the unsaturated zone provide an apparent cohesion over and above the effective cohesion, and thus, greater shearing resistance. This is often manifested in steeper bank slopes than would be indicated by ϕ'. Negative values of ψ equate to positive values of pore-water pressure (μ_w) and consequently, a reduction in shear strength. To quantify the magnitude of this effect, data are required on pore-water pressure distributions

in the bank. To address this data need, a field monitoring station has been established on Goodwin Creek, an incised channel in northern Mississippi that has been intensively studied by the National Sedimentation Laboratory of the US Department of Agriculture, Agricultural Research Service. Previous studies pertaining to channel and bank stability, and that describe the valley deposits can be found in Grissinger et al. (1981), Thorne et al. (1981), Little (1982), Grissinger and Murphey (1983, 1989) and Murphey and Grissinger (1985).

4.3. Hydraulic forces

Processes occurring at the bank toe are central to the understanding of bank failures and the evolution of bank morphology through time (Thorne, 1982). During degradational phases of channel evolution, bank heights are greater and bank surfaces below riparian tree roots become exposed. Consequently, in situ bank-toe material is more susceptible to basal erosion than in a non-incised channel. Shear stresses of low and moderate flows are also generally greater than in the non-degraded channel because of greater flow depths for a given discharge (Simon, 1992; Simon and Darby, 1997a). As flow stresses increase during the rising limb of a storm hydrograph, bank-toe erosion generally occurs previous to and out-of-phase with the maximum gravitational stresses imposed on the upper part of an incised streambank. Bank-toe erosion causes steepening of the bank profile, the possible formation of a cantilever, and the potential for destabilization of the remainder of the bank.

The erodibility of the bank-toe region can be expressed in terms of the relation between the resistance of in situ or failed bank-toe material with the hydraulic forces applied by the flow. Hydraulic stress is expressed here as mean boundary shear stress and is used as a measure of the erosive capability of the flow:

$$\tau_o = \gamma_w R S_w \tag{5}$$

where τ_o = mean boundary shear stress (N/m^2), γ_w = unit weight of water (N/m^3), R = hydraulic radius (m) and S_w = water-surface slope.

The resisting forces at the bank toe can be represented with a Shields-type critical shear stress. We have used a criterion developed by Wiberg and Smith (1987) for estimating the nondimensional critical shear stress (τ_{cr}^*) required to entrain blocks of failed cohesive bank material. This analysis is a physically based method designed to be used for poorly sorted (mixed-size), non-cohesive sediment particles that can also account for variations in particle density. τ_{cr}^* is obtained graphically using a nondimensional particle diameter (K^*) as the abscissa in a Shields-type entrainment curve where τ_{cr}^* is the ordinate (Wiberg and Smith, 1987):

$$K^* = 0.0047(\zeta^*)^{1/3} \tag{6}$$

where K^* = bed roughness length (k_s) for sediment of specific gravity 2.65 and fluid temperature of 10°C; and

$$\zeta^* = \frac{D^3(\rho_s - \rho)g}{\nu^2 \rho} \tag{7}$$

where D = representative particle diameter (m); ρ = fluid density (kg/m^3); ρ_s = sediment density (kg/m^3); g = acceleration due to gravity (m/s^2); ν = kinematic viscosity (m^2/s).

The nondimensional parameter (K^*) is a function of grain size, particle density, fluid density and viscosity such that any grain will have a unique value of ζ^* in a particular fluid environment. The factor $3.5 * D_{84}$ of the substrate is used for k_s in calculations of D/k_s to select the appropriate Shields-type curve for obtaining τ_{cr}^* (Wiberg and Smith, 1987), where D_{84} is the diameter of which 84% of the distribution is finer. Thus, a series of Shields-type entrainment functions are available based on the values of D/k_s. The conventional Shields entrainment function for uniform-sized particles is expressed as a curve with a value of D/k_s = 1.0.

To account for the fact that the particles rest on an inclined bank, an adjustment (Lane, 1953) is made such that:

$$\tau_{cb}^* = \tau_{cr}^* \cos\varepsilon \sqrt{\left[1 - \left(\tan^2\varepsilon/\mu^2\right)\right]} \tag{8}$$

where τ_{cb}^{*} = dimensionless critical shear stress on the side slope; ε = side-slope angle of the bank on which the failed material is deposited and μ = Coulomb coefficient of friction based on the assumption that it is equivalent to the tangent of the friction angle of the sediment ($\tan\phi'$) (Bagnold, 1953, 1966; Francis, 1973). Dimensionalized critical shear stress values are then obtained using the conversion:

$$\tau_c = \tau_{cb}^{*}\left((\rho_s - \rho)gD\right) \quad (9)$$

where τ_c = critical shear stress (N/m^2).

Eq. (8) is only applicable where the side-slope angle (ε) is less than the friction angle (ϕ'). However, packing, matric suction and cementation can result in side-slope angles being steeper than the friction angle. This is often the case for in situ bank-toe material in incised channels. In this case, a modification proposed by Millar and Quick (1993) and based on empirical evidence of the steepest angles measured in the field (ϕ^{*}) is applicable:

$$\tau_{cb} = 0.067\tan\phi^{*}\sqrt{\left[1 - (\sin\varepsilon/\sin\phi^{*})^{2}\right]} \times\left[(\rho_s - \rho)g\right]D_{50} \quad (10)$$

where D_{50} = median size of the sediment (m).

The value of this equation, however, is limited because of numerical problems when ϕ^{*} approaches the vertical because $\tan\phi^{*}$ becomes indeterminate. This is in the very range of ϕ^{*} that is common in the bank-toe region and the most critical for estimating the stability of the bank toe.

4.4. Study area

To better understand the interaction of hydraulic forces acting on the bed and bank toe, with the geotechnical forces acting on in situ bank materials in incised channels, a site with actively failing banks was selected for detailed study. Research was conducted in layered cohesive bank materials along the outside bend of a developing meander in Goodwin Creek, northern Mississippi (Simon and Darby, 1997b; Simon and Curini, 1998). A similar research site on the Sieve River, Italy is reported in Casagli et al. (1997, 1999) and in Curini (1998).

Along Goodwin Creek, MS, bank materials consist of about 2 m of moderately cohesive brown clayey-silt of late Holocene (LH) age (LH unit) overlying 1.5 m of early Holocene (EH) gray, blocky silt of low cohesion and lower permeability (EH unit). The post-settlement alluvium described by Grissinger and Murphey (1983) is contained within the LH unit. These units are separated by a thin (10–20 cm) layer containing manganese nodules and characterized by very low permeability, which tends to retard the downward movement of water. These materials overly 1 m of sand and 1.5 m of packed (often weakly cemented) sandy gravel. Bed material is bi-modal sands and gravels with a median bed-material particle size of about 9 mm.

5. Interaction of bed and bank processes

5.1. Evaluation of geotechnical forces

Apparent cohesion (c_a) and effective friction angle (ϕ') were measured in situ using an Iowa Borehole Shear Tester (BST; Luttenegger and Hallberg, 1981). Continuous measurement of pore-water pressures at five depths (0.3, 1.48, 2.0, 2.7 and 4.3 m) was undertaken with 5 pressure-transducer tensiometers along a 4.7-m high unstable streambank starting in November 1996. The tensiometers are subsequently referred to as T-30, T-148, T-200, T-270 and T-433, respectively. Data from the tensiometers are supported with data from a pressure transducer housed in a pipe attached to the streambank to record surface-water stage in the channel and to calculate confining pressures. All instruments provide data at 10-min intervals.

A series of 16 BST tests was conducted in the LH unit around an additional tensiometer placed at a depth of 1 m in the center of a circular area. BST tests were then carried out at a depth of about 1 m over a range of soil-moisture conditions. This was done to provide data to evaluate the angle ϕ^{b}, which represents the rate of increase in shear strength due to matric suction. By Eq. (4), this also provides field-based estimates of effective cohesion. Matric suction varied between 3.3 and 31.0 kPa for the BST tests. Results revealed an apparent cohesion varying between 0.0 and 8.4 kPa and an average effective

friction angle of 28.1°. Ten BST tests taken between June 1996 and July 1998 in the underlying EH unit disclosed apparent cohesion values varying between 0.0 and 37.9 kPa and an average effective friction angle (ϕ') of 28.5° (Table 1).

Undisturbed cores were collected to evaluate the relation between γ and matric suction (ψ) for each bank material unit. For the LH unit, values of γ range from 16.2 to 18.1 kN/m^3 depending on the degree of saturation (Fig. 1A). A soil–water retention curve expressing the relation between θ and matric head (h_m; in cm) was developed from the data (Fig. 1B). Results taken during a drying phase show a trend characteristic of a fine material as evidenced by the relatively high moisture contents (28–39%) for corresponding values of matric head (up to 310 cm; Fig. 1B). The results of the in situ measurements are summarized in Table 1.

5.2. Evaluation of ϕ^b

At the time of writing (1998) we are not aware of any laboratory or field data on the parameter ϕ^b for alluvial channel materials. Reported values are applicable only to tropical hillslope materials (Fredlund and Rahardjo, 1993). To evaluate ϕ^b in the LH unit, values of apparent cohesion were plotted against matric suction (Fig. 2). Considerable data scatter exists for suction values less than 8.0 kPa. This occurs because ϕ^b varies with matric suction from its maximum at saturation ($\phi^b = \phi'$) and decreases with increasing matric suction until ϕ^b reaches a steady value (Fredlund and Rahardjo, 1993). Only values greater than 8.0 kPa are included in the relation shown in Fig. 2 because ϕ^b reaches a steady value in this domain. The value of ϕ^b for the LH unit derived by linear regression is 10.4°. Because $\tan(10.4°) = 0.184$, by Eq. (4), this indicates that a matric-suction value measured in the LH unit translates to a value of apparent cohesion due to matric suction of about 18% of the measured value. Extrapolation of the regression relation between ψ and ϕ^b results in a y-intercept and value of c' equal to about 2.7 kPa (Fig. 2).

Increments of shear strength, such as those due to matric suction, are most important under moisture conditions close to saturation. It is meaningful, therefore, to attempt to define ϕ^b and its effects on apparent cohesion in the very range of ψ values where it varies rapidly and is the most difficult to do so. For the conditions at the Goodwin Creek streambank, this range has been shown to be $0 < \psi < 8$ kPa. Field data provide two fixed points for ϕ^b, 28.1° at $\psi = 0.0$ kPa and 10.4° at $\psi = 8.0$ kPa. The effect of varying ϕ^b on apparent cohesion is tested by providing different models representing the behavior of ϕ^b within the specified range of ψ (Fig. 3A).

Local peaks in apparent cohesion are obtained in the range $0 < \psi < 8$ kPa when assuming the type of relation proposed by Fredlund and Rahardjo (1991), where $\phi^b = \phi'$ for matric-suction values increasing from zero, and then drops to its steady value at a certain value of matric suction (ψ_{drop}) (Fig. 3B). This point coincides with the air-entrainment threshold of the material. In laboratory experiments with unsaturated glacial till, ψ_{drop} occurred at about 100 kPa (Gan and Fredlund, 1988), 60 kPa for a clay compacted to a high density and 25 kPa for a clay compacted to a low density (Fredlund et al., 1987). These ψ_{drop} values are well outside the range specified for the Goodwin Creek material. We specified ψ_{drop} values of 0.0, 1.5, 3.5 and 5.0 kPa and rates of

Table 1
Geotechnical characteristics of in situ bank materials

Study site	c_a (kPa)	ϕ' (degrees)	ϕ^b (degrees)	γ (kN/m^3)	z_{calc} (m)
Goodwin-LH unit	0.0[a]–8.4	28.1	10.4	16.2–18.1	4.2
Goodwin-EH unit	0.0[a]–37.9	28.5	17.5[b]	17.1–19.1	1.1
Goodwin-sand unit	0	32.8	17.5[b]	17.1	–

LH = late Halocene; EH = early Halocene.
[a] 0.0 values are suspect.
[b] Equals assumed average value.

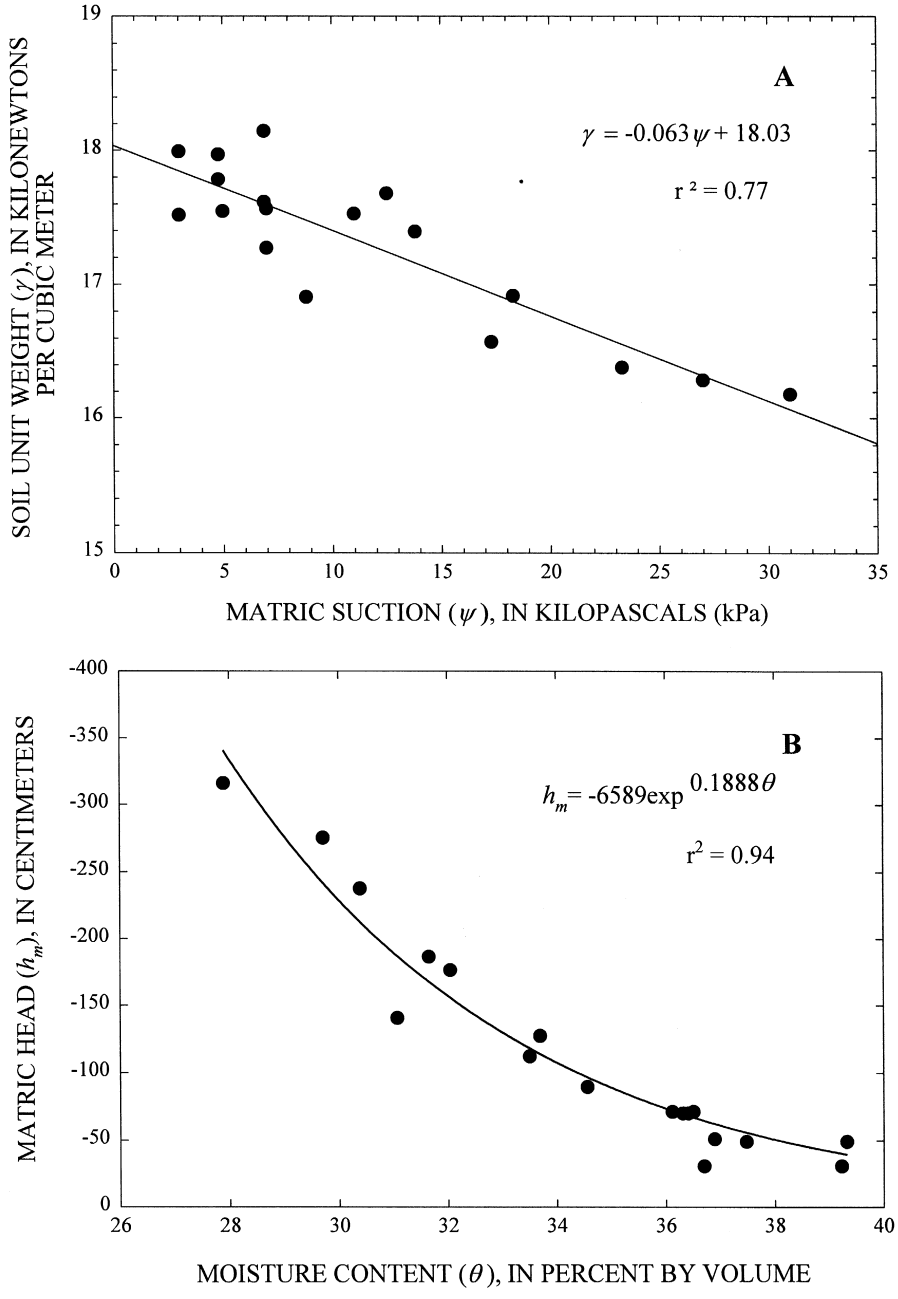

Fig. 1. Relation between soil bulk unit weight and matric suction in the LH unit (A) and soil–water retention curve for the LH (silty) unit on Goodwin Creek (B). Note that values of θ in the regression equation are expressed as a fraction.

drop (χ) of 4, 6 and infinite degrees/kPa, thereby producing local extremes of c_a at ψ values ranging from 3.5 to 8.0 kPa. The model assumed by our determination of c' from ϕ^b above, implies that ϕ^b drops drastically from ϕ' (28.1°) to 10.4° for any matric-suction value greater than 0.0 kPa (line repre-

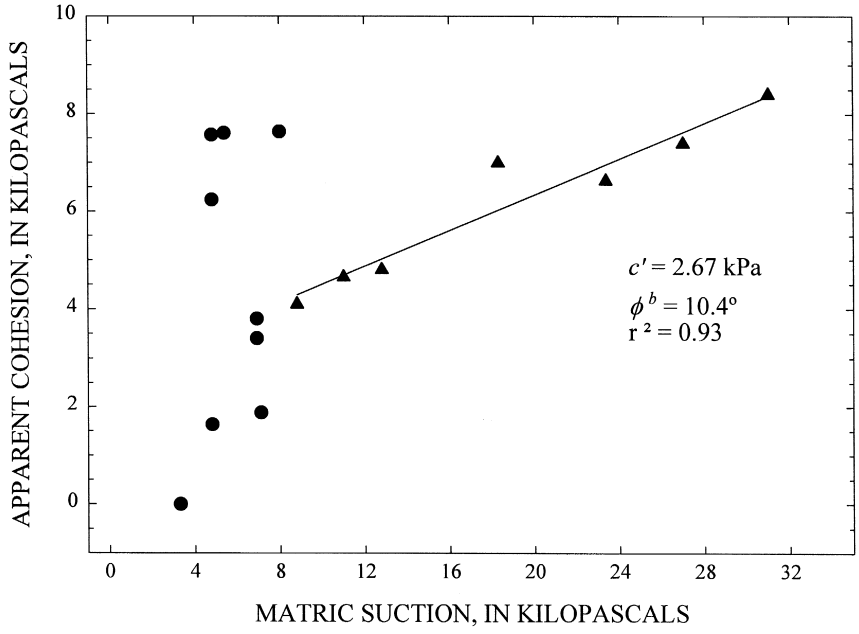

Fig. 2. Derivation of the parameter ϕ^b from in situ shearstrength determinations in the LH (silty) unit on Goodwin Creek over a range of matric-suction values. Note that only datapoints shown as triangles are included in the regression relation.

sented by $\psi_{drop} = 0.0$ and $\chi =$ infinite in Fig. 3A). Values of c_a assuming this model (constant ϕ^b) are represented by the linear function in Fig. 3B. Alternatively, assuming a linear relationship where $\phi^b = 28.5 - (28.5 - 10.4), \psi/8$ produces a local extreme at $\psi = 6$ kPa. The existence of local extremes due to increasing values of ϕ^b implies that magnitudes of apparent cohesion can be similar to those at greater values of matric suction and that there exists an optimum ψ value in the moisture-content domain close to saturation. The magnitude of this local extremum in apparent cohesion is significantly affected by ψ_{drop}. However, determination of c' remains unaffected by the selection of the model. The envelope described by the bounding relations in Fig. 3B represents the expected range of apparent cohesion values.

5.3. Conditions of bank failure

Four major failure episodes occurred at the Goodwin Creek research site between February and December, 1996, resulting in up to 2 m of top-bank retreat. This rate is greater than the 30-year average of about 0.5 m/year as determined using dendrochronologic evidence from riparian trees (Simon and Darby, 1997b). Higher than average bank retreat during the study period may be attributed to persistent precipitation, manifest in 10 discharge peaks with a 1-year recurrence interval or greater. Additional failures occurred during September 1997, January 1998 and March 1998. Each failure episode occurred during recession of stormflows; one occurring more than 24 h after recession. Planar and cantilever failures were relatively common along the steepest section of the 4.7-m high banks. Cantilevers were formed by two processes. First, preferential erosion of sands and silts by fluvial undercutting about 3.0–3.5 m below the top bank. Second, by sapping and small pop-out failures in the region of contrasting permeabilities in the Holocene units about 1.6 to 2 m below the top bank. Both of these processes resulted in oversteepening at the base of the EH unit and subsequent collapse during wet periods.

Results revealed that the loss of matric suction from infiltrating precipitation and subsequent vertical

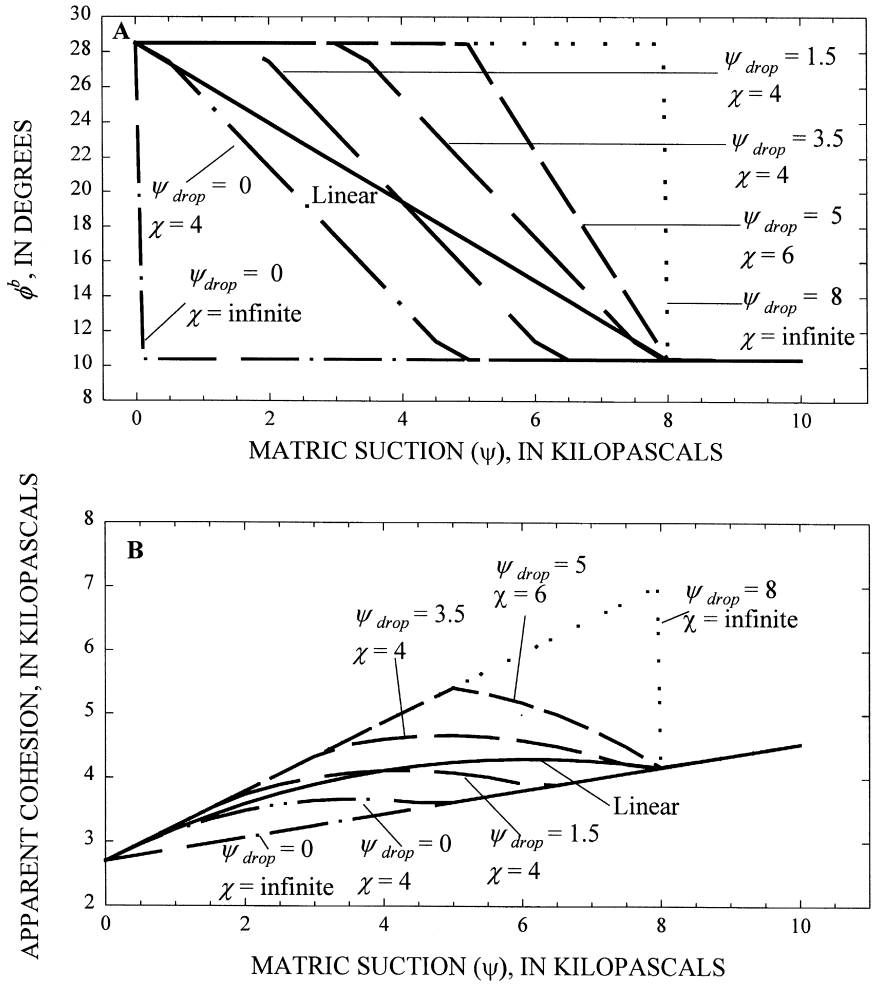

Fig. 3. Relation between matric suction (ψ) and ϕ^b for various rates and styles of decreasing ϕ^b, from $\phi' = 28.1°$ at $\psi = 0.0$ kPa to 10.4° at $\psi = 8.0$ kPa (A) and corresponding effects on values of apparent cohesion (B). Note: ψ_{drop} = point where ϕ^b begins to decrease; χ = rate of decrease in degrees per kilopascal.

seepage may be as significant as the development of positive pore-water pressures in contributing to mass-bank instability and, therefore, plays an important role in bank stability. Large losses (of at least 50%) of matric suction in the upper part of the Goodwin Creek bank are common in response to only moderate amounts of rainfall (about 2.5 cm) and 1.0 m rises in stage during the winter months. Fig. 4 shows reduction of ψ and shear strength at a depth of 0.3 m began at about 1300 h on November 29, 1996 in response to precipitation. Stage began to rise at about 0200 h on November 30 but reductions in matric suction at a depth of 1.48 m did not start until 0800 h. The complete loss of 2–4 kPa of matric suction combined with reduction in matric suction from 12 to about 5 kPa in the upper meter of bank and the generation of 5 kPa of excess pore-water pressure at 2.0 m resulted in mass failure of the bank on November 30, 1996 at 1101 h. The precise moment of failure is known because collection of reliable stage data was interrupted when the bank supporting the stage-recording transducer failed. At

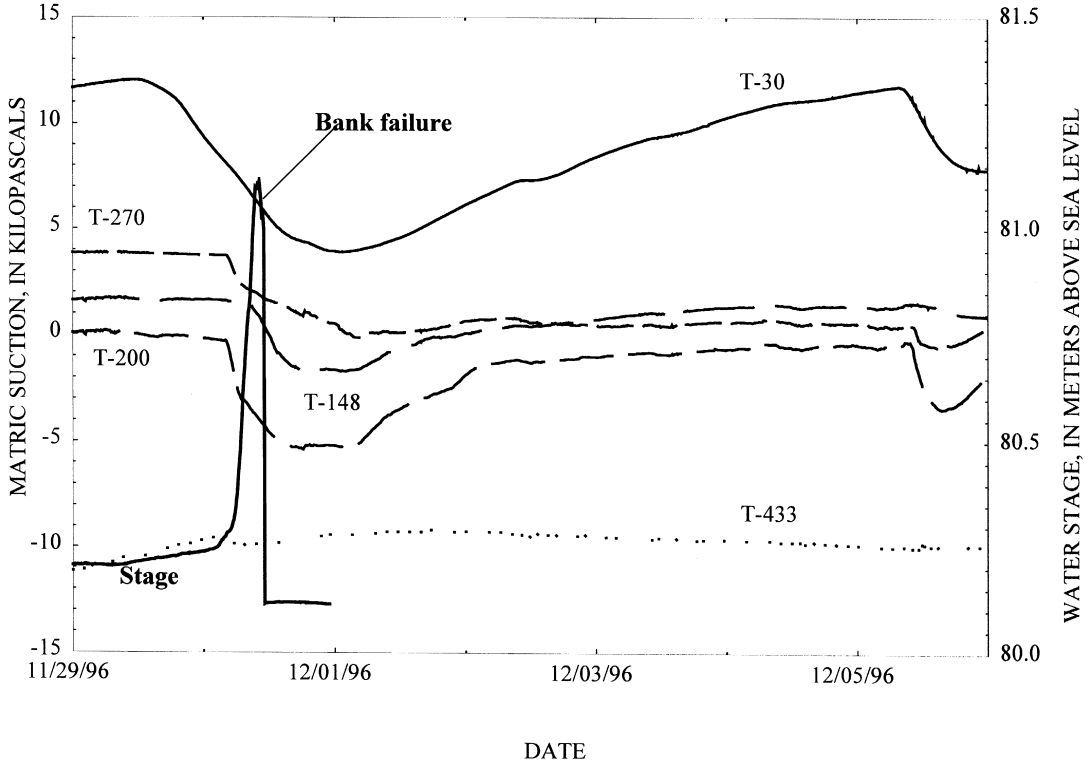

Fig. 4. Variation in matric suction during storm of November 30, 1996 at Goodwin Creek showing moment of bank failure.

the moment of failure, only the upper 0.5 m of the bank provided consequential amounts of matric suction to enhance cohesion and shear strength.

As another example, a series of moderate precipitation events (2.5–5 cm) induced eight successive moderate rises in stage (1–2 m) on Goodwin Creek during January and February 1998 (Fig. 5). Bank failures did not occur, however, until after recession of the third storm (January 13, 1998) when individual matric-suction values were close to minimums for all the tensiometers (Fig. 5B). ψ values of 13 kPa in the LH unit were diminished to about 5 kPa. ψ values of 4 kPa in the EH were eliminated ($\psi = 0.0$) with saturation reaching the 2.0-m level and positive pore-water pressure of 4 kPa at a depth of 2.7 m. Assuming an average ϕ^b value of about 17.5° (Fredlund, 1986), cohesion due to matric suction was thereby reduced from about 4.1 to 1.6 kPa in the upper LH unit and eliminated entirely in the lower EH unit. Applied over the length of the failure plane, cohesion due to matric suction fell from about 4.5 to less than 1.0 kN/m (Fig. 5C). The proportion of shear strength due to matric suction acting on the failure surface during this period thus decreased from about 17% to a minimum of 4% at the time of failure (Fig. 5D). The strong unidirectional adjustment of the 2.7-m tensiometer (T-270) indicates the steady downward movement of water (vertical seepage) from the perched layer as a consequence of a continuous supply from the LH unit above. In this case, bank instability was induced only after water had been able to move through the thin layer of manganese nodules atop the EH unit and penetrate deep into the EH unit. Integrated over the length of the failure plane (which includes all three units), cohesion due to matric suction was at a minimum at the time of failure (Fig. 5C).

The rapid responses of the 0.3-m tensiometer (T-30) and the hysteresis effect demonstrated by the more rapid wetting phase compared to the drying

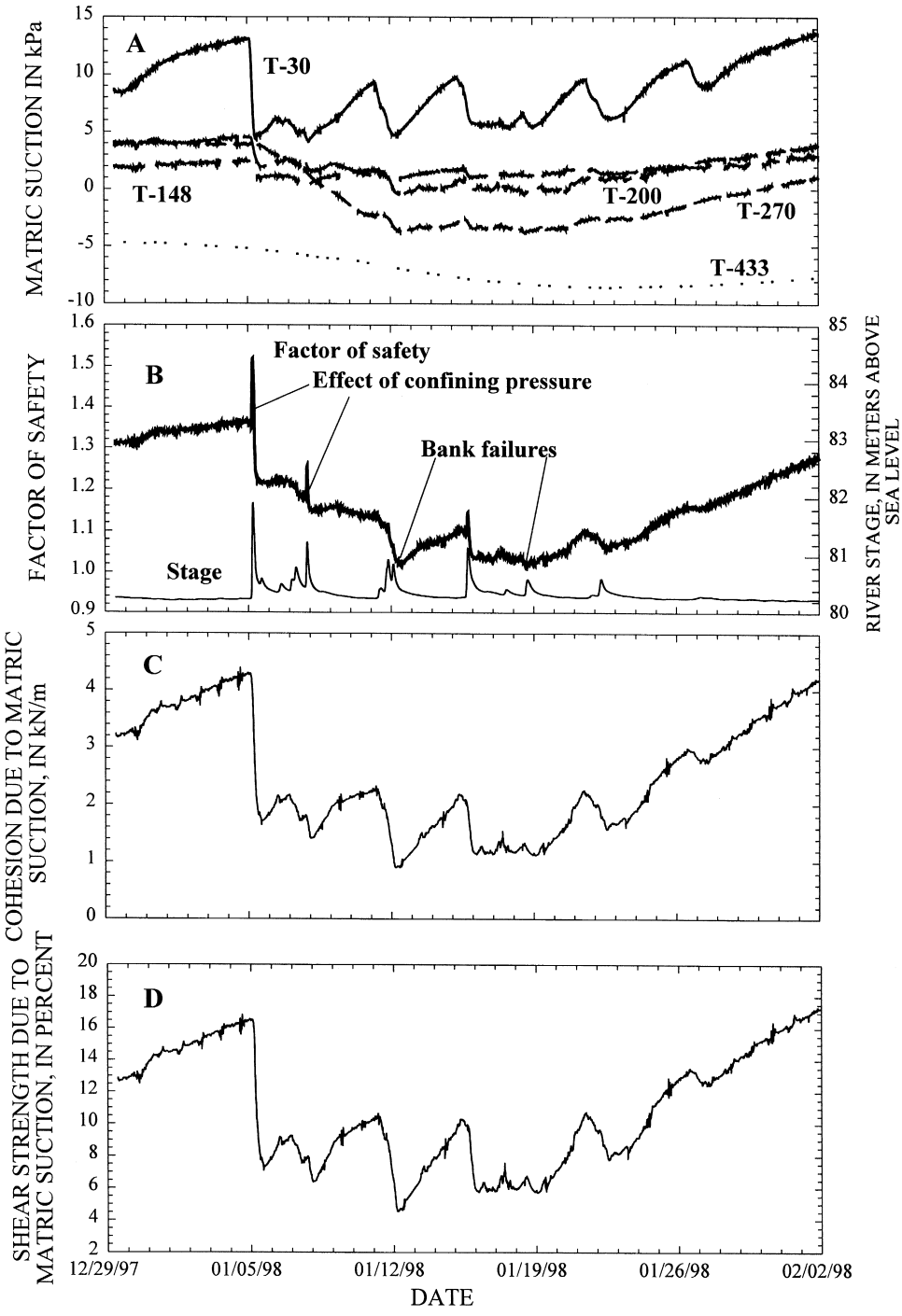

Fig. 5. Variation in matric suction during storms of January–February 1998 at Goodwin Creek (A), factor of safety from Eq. (11) and river stage showing bank failure during recession of third storm (B), percent of apparent cohesion acting on the failure plane due to matric suction (C) and percent of shear strength due to apparent cohesion (D).

phase can clearly be observed (Fig. 5A). This effect in combination with low permeabilities helped to create the lag times recorded by the tensiometers at different depths. The period of January 8–11 shows distinct drying (Fig. 5A) representing a loss of hydraulic head (or stage) (Fig. 5B) in the LH unit (T-30 and T-148) during the dry days following the January 8 storm event. In contrast, the deeper tensiometers in the EH unit (T-200 and T-270) are showing decreases in matric suction representing increases in hydraulic head (stage) during this same period, representing the wetting phase of the same January 8 storm.

5.4. Numerical analysis of bank failure

A bank-stability algorithm for cohesive layered banks was developed incorporating both the failure criterion of Mohr–Coulomb for the saturated part of the failure surface, and the failure criterion modified by Fredlund et al. (1978) for the unsaturated part of the failure surface. The algorithm, based on the Limit Equilibrium Method, accounts for several additional forces acting on a planar failure surface including the:

1. force produced by matric suction on the unsaturated part of the failure surface (S);
2. hydrostatic-uplift force due to positive pore-water pressures on the saturated part of the failure plane (U), and
3. hydrostatic-confining force provided by the water in the channel (P)

(Casagli et al., 1997, 1999; Curini, 1998; Simon and Curini, 1998). Here, multiple layers are incorporated through summation of forces in a specific (ith) layer acting on the failure plane. Increases in γ due to increases in moisture content from vertical or lateral seepage have been seen to be important in calculations of the downslope component (W). This effect has been incorporated dynamically into the F_s algorithm by including the moisture-content/soil unit weight relation for the upper, LH unit. A refined set of results would be obtained by including the moisture-content/soil unit weight relation for the lower EH unit as well as for the basal sand–gravel unit. The factor of safety (F_s) is given by:

$$F_s = \frac{\Sigma c'_i L_i + (S_i \tan \phi_i^b) + [W_i \cos \beta - U_i + P_i \cos(\alpha - \beta)] \tan \phi'_i}{\Sigma W_i \sin \beta - P_i \sin(\alpha - \beta)} \quad (11)$$

where L_i = the length of the failure plane incorporated within the ith layer; S = the force produced by matric suction on the unsaturated part of the failure surface (kN/m); U = the hydrostatic-uplift force on the saturated portion of the failure surface (kN/m); and P = the hydrostatic-confining force due to external water level (kN/m). Eq. (11), a new algorithm, represents the continued refinement of bank-failure analyses by incorporating additional forces and soil variability (Osman and Thorne, 1988; Simon et al., 1991; Casagli, 1994; Darby, 1994; Rinaldi, 1994; Casagli et al., 1997, 1999; Curini, 1998; Simon and Curini, 1998).

The forces operating on the Goodwin Creek bank and parameter values are shown in Fig. 6. The shape of the failure surface was obtained from surveys made before and after the bank failures that occurred in January 1998. Examples of the change in bank morphology over much of the monitoring period are shown in Fig. 6C. The change in morphology between the February 1996 and July 1997 surveys represent a series of mass-wasting events. Erosion between July and October 1997 represents a discrete event in September 1997. The failure-plane angle (α) was 79°. Because of the lack of data for the middle and lowest part of the bank, an average value of 17.5° for ϕ^b was used. A ϕ^b value of 10.4° based on measured data was used for the upper portion of the failure surface (Figs. 1A and 6A).

The algorithm utilizes values measured from the Goodwin Creek tensiometer/pressure-transducer array installed near the bank edge, resulting in a dynamic assessment of bank-stability conditions as hydrologic conditions change. Data from the tensiometers are weighted according to their location relative to the failure plane and applied to calculations of driving and resisting forces. Minimum factors of safety (F_s about 1.0) are calculated to occur during the period when mass failures were observed in the field after the storm events (Fig. 5B). During winter periods, such as those shown in Figs. 4 and 5,

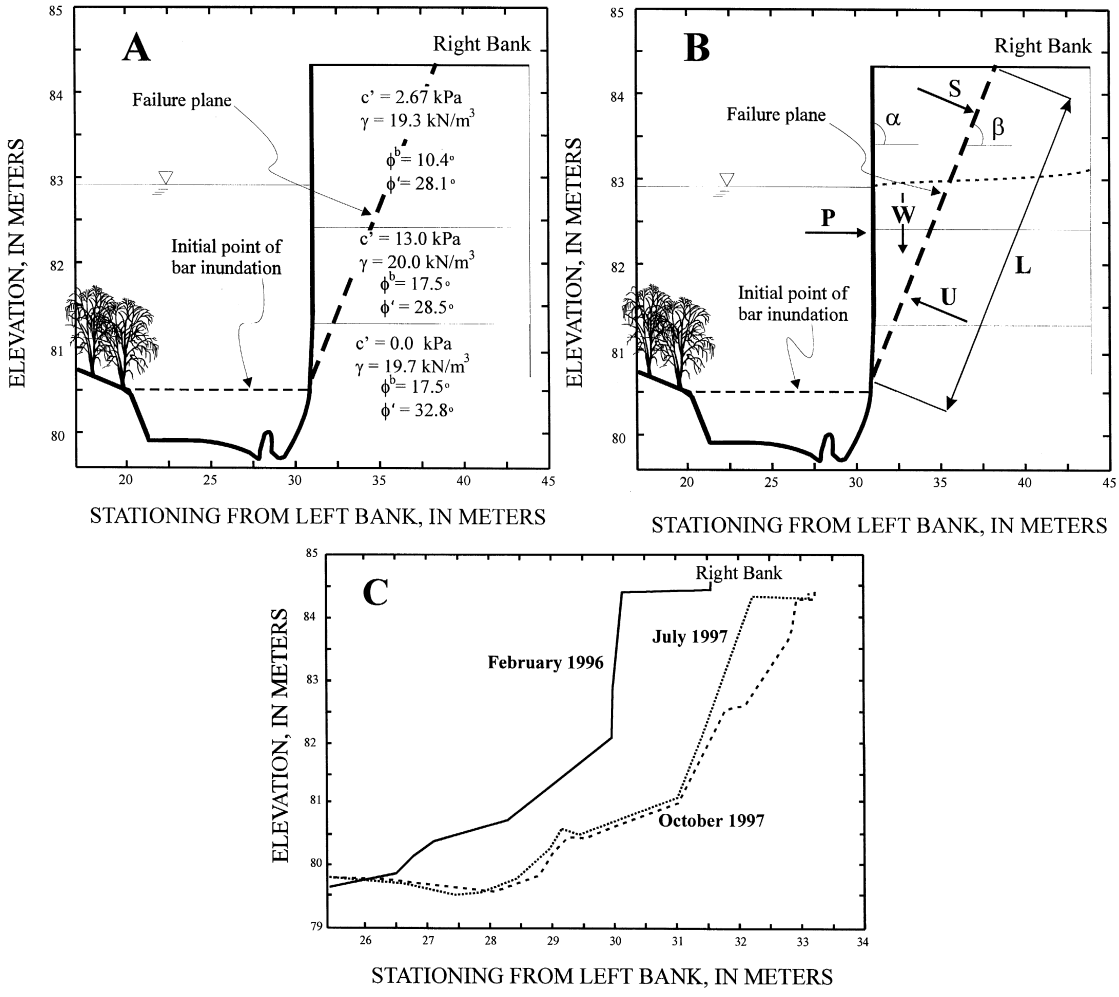

Fig. 6. Geometry of the Goodwin Creek streambank showing parameter values and failure plane (A), forces considered in Eq. (11) (B) and selected time–series cross sections (C).

matric suction is shown to account for a small to moderate (4–20%) but important amount of shear strength (Fig. 5D). The factor of safety changes as a consequence of suction, pore-water pressure and river-stage fluctuations (confining pressure). Abrupt changes of F_s depend on rapid rises in river stage. During these periods, the confining pressure increases, producing a sharp peak in the factor of safety (Fig. 5B). During recession of river stage, the confining pressure decreases rapidly causing a decrease of the factor of safety. If this loss in confining pressure is associated with a simultaneous decrease in matric suction produced by the continued downward movement of a wetting front, a minimum F_s can be obtained (Figs. 5 and 7). Essentially, it is the discrepancy between the rate of change of forces operating in the channel and those operating within the bank that cause out-of-phase hydrologic adjustments, worst-case (rapid-drawdown) conditions, minimum F_s and as a consequence, bank failures.

5.5. Interpretation and summary of modeling results

The bank-stability algorithm developed here has been successful at modeling bank failures and determining the role of matric suction on bank strength

and stability. Simulations of bank-stability conditions were able to provide extremely close correspondence between the timing of modeled and observed failures. The data collected at the tensiometer measuring station show the temporal variability of seepage forces and the lag time inherent in reductions in shear strength due to losses of matric suction and generation of positive pore-water pressures. The results indicate that it is not necessarily the largest storms and greatest floods that induce bank failures, but prolonged wet periods such as January 4–22, 1998 (Fig. 5), in which matric suction diminished, soil unit weight increased and positive pore-water pressures developed. This occurred as a consequence of vertical seepage due to rainfall, sub-horizontal seepage of water from the drainage basin and preferential movement of water along cracks formed from tension, living and decayed roots, structural weaknesses, or desiccation. Horizontal seepage from the river into the bank did not appear to be significant at the Goodwin Creek site because of the rapid rise and fall of storm hydrographs. Curini (1998) indicates that in more permeable materials such as along the Sieve River, Italy, seepage from the river into the streambank can also be important in reducing matric suction during and soon after periods of high flow.

5.6. Seasonal variations in bank strength and bank stability

Continuous tensiometer measurements taken over the study period provide direct evidence of strong seasonal variations in bank strength and bank stability (Fig. 7). The general increase in matric-suction values from May to July 1998 is readily apparent from the trends shown for individual tensiometers (Fig. 7A). As expected, variations are greatest for those instruments closest to the ground surface (T-30). The seasonal variations shown in Fig. 7A are not as great as those reported by Casagli et al. (1997) and Curini (1998) for a more permeable incised streambank in Tuscany, Italy. High temperatures, high rates of evapotranspiration and a dearth of intense precipitation events combined with moderate permeability to result in matric-suction values as high as 85 kPa (air-entry level of the tensiometer cups). Summer matric-suction values in the cohesive Goodwin Creek bank do not reach 85 kPa notwithstanding the generally hot conditions in the southeast United States during the summer. Maximum values recorded at depths of 0.3 m (T-30) reached about 60 kPa during July 1998 although it is conceivable that values of 85 kPa are attainable. At 1.5 m (T-148), values reached 35–40 kPa (Fig. 7A). These values of matric suction correspond to a maximum cohesive strength due to suction at 1.48 m of 7.3 kPa (assuming $\phi^b = 10.4°$). However, it is the cohesion imparted to the streambank by matric suction during the wetter winter months that is critical in determining the stability of a streambank in an incised channel.

During the rainy season, which generally occurs in winter and spring, individual tensiometers show matric-suction values between 0.0 to about 18 kPa, with the shallowest instrument (T-30) recording the highest values (Fig. 7A). During rain-free periods of winter and spring, cohesion due to matric suction acting on the failure surface is about 5 kN/m (Fig. 7C) which represents about 20% of the shear strength along the potential failure surface (Fig. 7D). Periods of wet weather during this time of the year are critical because cohesion acting on the failure plane due to matric suction drops to near 0.0 kN/m (Fig. 7C and D). However, if the shear strength imparted to the streambank by suction or other forces is sufficient to resist mass failures during this period, it is likely that the banks will remain stable for the remainder of the year. Summer convective storms simply do not deliver a sufficient amount of water over an extended period of time to wet streambanks adequately to cause large enough losses in matric suction and cohesion to produce F_s values less than or near 1.0 (Fig. 7). This can be seen for the storms (flow events) in late spring (May and June 1998) in which significant losses of matric suction only occur within the upper 1.5 m of the bank (Fig. 7). At depths of 2–4 m, the bank is not largely affected. After May 1998, F_s values depart from the general 1.0–1.5 range that is characteristic of the winter and spring months, and increase towards 3.0 as the bank begins to dry and matric suction and shear strength increases (Fig. 7).

Except for summer periods, soil water flow is directed from the top of the bank to the groundwater table as a consequence of the continuous supply provided by precipitation and because of low rates of

evapotranspiration. Matric-suction values generally increase from the groundwater table at about 4.2–0.3 m (Fig. 7A). During the summer months, however, the direction of water flow within the bank can shift from downward to upward because evapotranspiration exceeds inputs of water from precipitation.

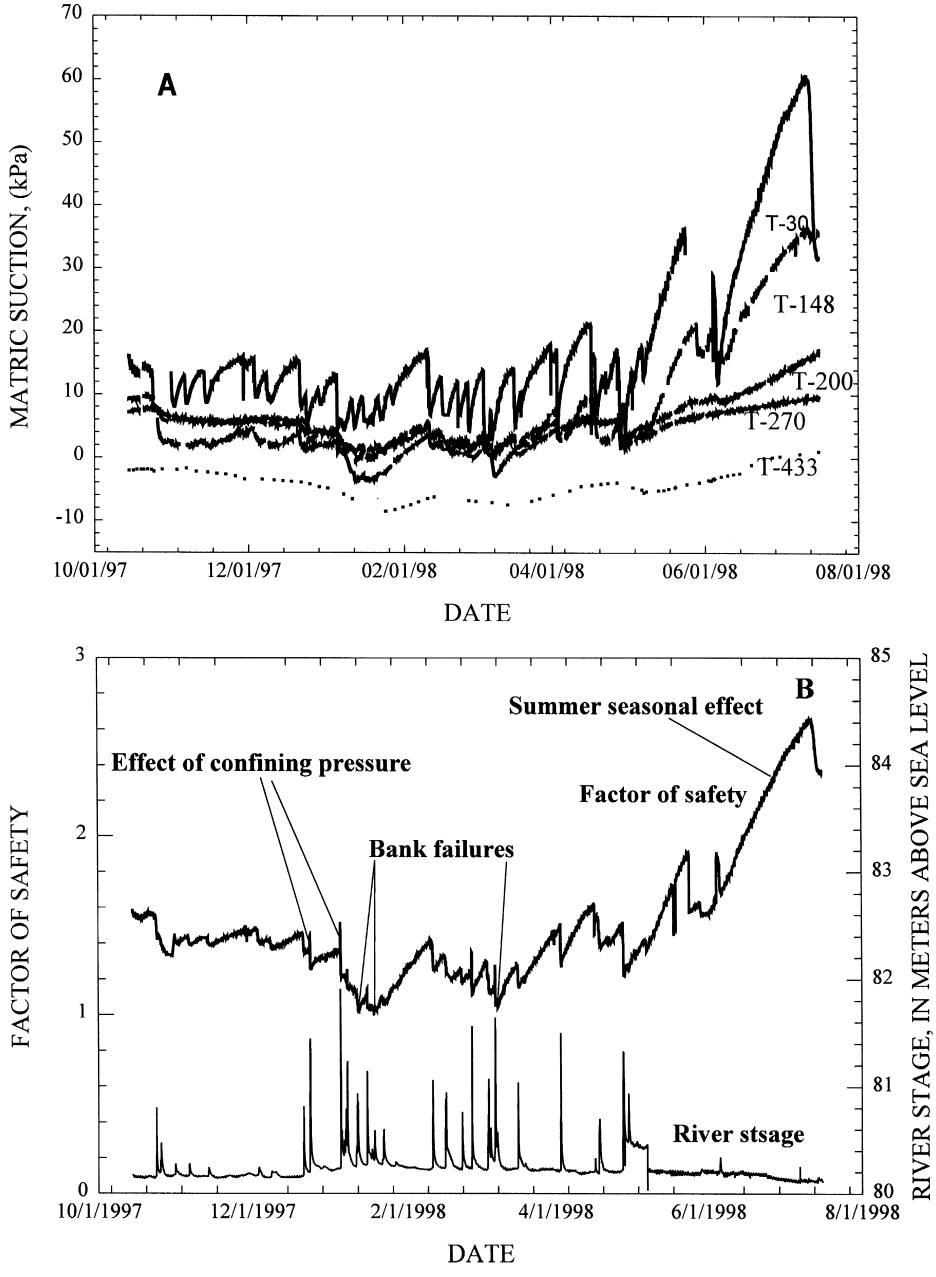

Fig. 7. Seasonal variations in matric suction (A), factor of safety using Eq. (11) and stage (B), cohesion due to matric suction acting on the failure plane (C) and shear strength due to matric suction (D) for the period October 1997 to July 1998.

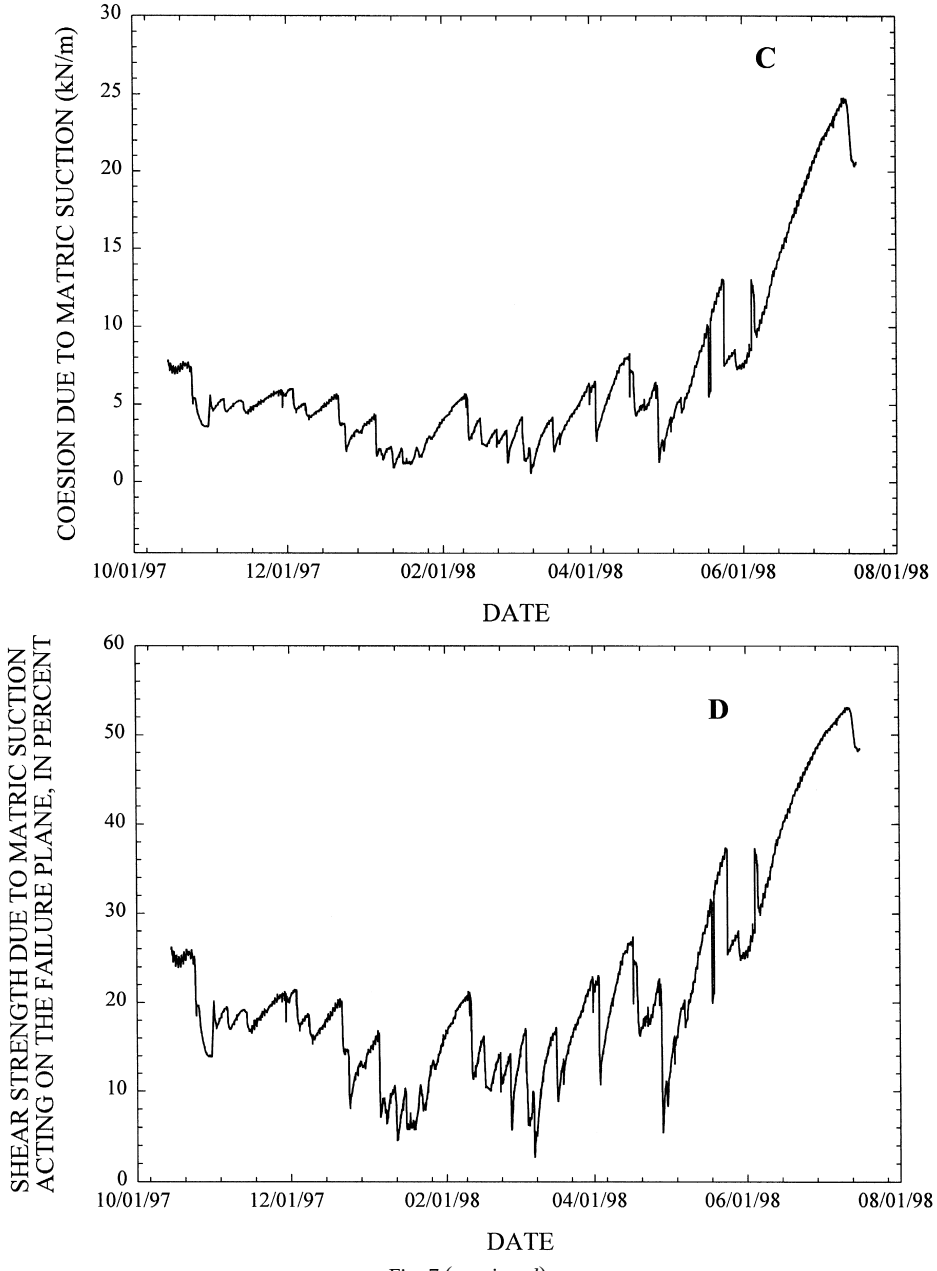

Fig. 7 (*continued*).

5.7. Hydraulic forces and processes

It has been shown how, for a given bank geometry, changes in bank hydrology can induce bank failure. Similarly, increases in bank height by bed degradation and bank angle by undercutting favor bank failure by causing the gravitational component to increase. This occurs through an increase in the gravitational force component acting on the in situ bank. When considering bank-toe erosion by hydraulic forces via undercutting, the opposing forces operating at the bank toe can be represented by the

shear stress provided by streamflow acting against the resistance of the bank-toe material to be entrained by the fluid. We must be able to account for the resistance of that basal material to erosion, be it in situ bank material, cohesionless bed material, or failed cohesive blocks. It is conceivable that a different set of parameters are required to account for the erosion resistance of each of these types of materials, particularly when the compounding effects of riparian vegetation are considered.

5.8. Conditions of bank-toe erosion

Fluvial erosion of bank-toe and in situ materials was measured on Goodwin Creek using a network of seven sets of erosion pins spaced longitudinally along the outer bank. Each set of pins is made up of three 60-cm long pins inserted horizontally into the bank-toe region and displaced vertically about 0.5 m apart. Pins were initially placed in failed, reworked, or in situ materials. Each pin was measured after 16 runoff events between February and December 1996. Lawler (1993) has reviewed advantages and limitations of erosion pins of this type. Based on measurements of protrusion lengths made by different operators on the same day, we estimate that erosion pin data are accurate to within ± 5 mm. Estimates of the change in length between visits are accurate, therefore, to within 1 cm. However, additional systematic errors may be introduced through the effects of (1) turbulent scour around the tip of the pins and (2) disturbance of the bank material fabric during insertion of the pins.

Individual flow events resulted in as much as 0.5 m of toe removal at and up to 2.7 m over the period February 1996 to July 1997 (Fig. 8). Erosive events are represented by the negative peaks in Fig. 8A and C and correspond to several peak-flow discharges with recurrence intervals between 1 and 1.5 years.

The erosional force provided by the flows is represented by peak-flow shear stresses at the bank toe. These were calculated from data obtained from crest-stage gages installed at the entrance and exit of the reach (Simon and Darby, 1997b):

$$\tau = \gamma_w (E_w - E_p) S_{wp} \quad (12)$$

where E_w = elevation of water surface at peak flow (m), E_p = elevation of erosion pin (m) and S_{wp} = peak flow water-surface slope. The greatest bank-toe shear stresses calculated from Eq. (12) were between about 30 and 50 N/m^2. Typically, however, the bottom pins, which experienced greater shear stresses, showed more erosion than middle or top pins, indicating a general steepening of the bank toe during stormflows (Fig. 8). This steepening primes the channel bank for the next mass failure, which can take place during the next loss of matric suction and occurrence of excess pore-water pressures.

Bank-toe erosion amounts are, in part, a function of the availability and sizes of failed bank material at the bank toe during runoff events, and therefore, erosion amounts were not similar for relatively similar stormflows and shear stresses. Cumulative plots of bank-toe erosion show the effects of decreasing rates of bank-toe erosion (Fig. 8B and D) as the supply of failed blocks decreases with time until a fresh failure supplies new blocks to the bank toe (Fig. 8D). Size distributions of the failed blocks and of in situ bank-toe material were determined from analysis of repetitive photographs of the bank-toe region taken after flow events (Table 2). Some blocks have weathered to half their original block size over a period of 5 months from the combined effects of runoff and raindrop impact, and over much shorter periods, by cracking.

To determine the conditions necessary to entrain failed cohesive blocks which have collected at the bank toe, the critical shear stress for the most common bank-toe conditions are determined using the Wiberg and Smith (1987) approach as well as the standard Shields criteria. The most common failure-block deposition scenarios in order of decreasing frequency are (1) EH blocks deposited on gravel-toe material, (2) LH blocks deposited on gravel-toe material and (3) LH blocks deposited on EH blocks. Estimated critical shear stresses for the range of D_{max} and k_s values are shown in Table 3. These estimates are based on values of $\varepsilon = 25°$ obtained from field surveys, and a friction angle of 35° ($\mu = 0.70$) used for Eq. (8). These values of ε and μ result in a correction factor of 0.68. Estimates for entrainment of the gravel-toe material are also provided.

The high critical shear stress value (183 N/m^2) determined for the smaller LH blocks deposited on EH material represents "hiding" between the larger

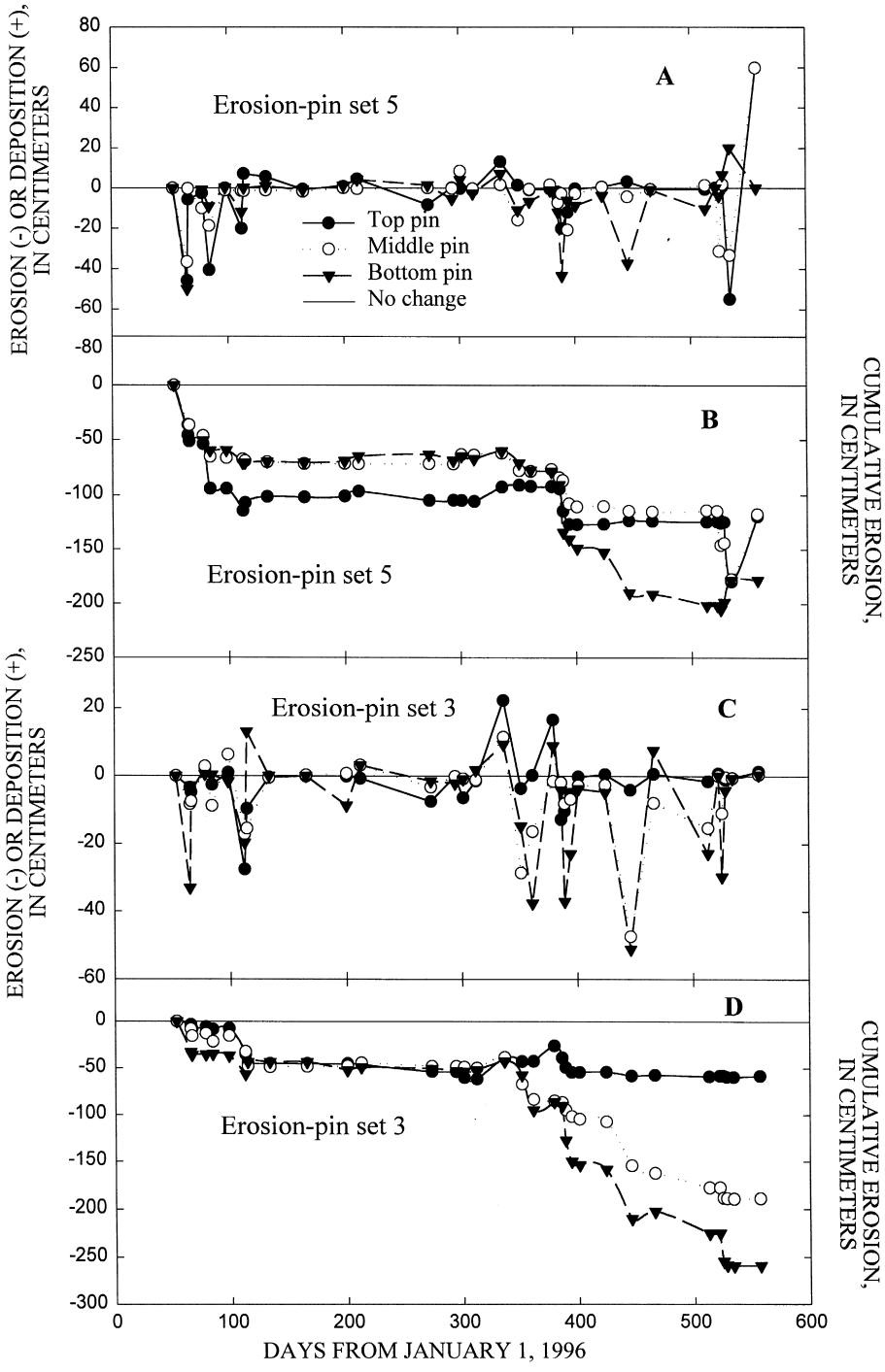

Fig. 8. Bank-toe erosion by hydraulic forces and deposition from failures at erosion pin sets 3 and 5 on Goodwin Creek showing individual events (A and C) and cumulative amounts (B and D).

Table 2
Representative particle sizes of freshly failed bank materials and gravel-toe material (Simon and Darby, 1997b)

Percentile	Failed LH		Failed EH		Gravel-toe material	
	Mean	n[a]	Mean	n[a]	Mean	n[a]
Largest (mm)[b]	364	7	639	6	97	8
D_{max} (mm)[c]	215	7	420	6	66	8
D_{84} (mm)	78	7	158	6	33	8
D_{50} (mm)	37	7	50	6	21	8
D_{16} (mm)	1	7	14	6	11	8
Mean (mm)	49	7	84	6	22	8

[a] n = number of observations (photographs).
[b] Largest = largest block observed.
[c] D_{max} = mean of five largest blocks.

EH blocks. However, LH materials failing vertically from cantilevers often are deposited atop failed blocks of EH material suggesting that τ_c for the LH materials are significantly overestimated by the Wiberg and Smith (1987) equations. Furthermore, it was found that calculated values of K^* exceeded the plotted bound of K^* to be used for the various D/k_s curves provided by Wiberg and Smith (1987). For this study, the maximum K^* value (5.0) was, therefore, used. Critical shear stress values (τ_c) for D_{max} obtained using a standard Shields approach a τ_{cr}^* value of 0.03 and the Lane (1953) correction (Eq. (8)) are 79.8 and 36.6 N/m^2 for the EH and LH units, respectively. The same analysis yielded critical shear stress values of 30.0 and 13.3 N/m^2 for the EH and LH D_{84} size fractions. For the cemented in situ sand and gravel unit at the bank toe, Eq. (10) produces $\tau_c = 39.0$ N/m^2 based on the following input values $\phi^* = 85°$ and $\varepsilon_c = 80°$.

Peak shear stresses at Goodwin Creek between about 30 and 50 N/m^2 were sufficient to entrain all LH materials on four separate occasions, all but the largest blocks of EH material, and localized areas of the in situ, cemented sand and gravel material. These shear stresses were associated with stormflows having 1.0–1.5 year recurrence intervals and flow depths to about 1.5 m. These results, combined with field observations, show that a Shields-type approach is applicable for analyzing entrainment thresholds of failed blocks of cohesive material. Entrainment of the largest EH blocks (about 639 mm) deposited on the gravel-toe material requires a shear stress of about 121 N/m^2, a flow that was considered likely within the incised channel. A 3-m deep flow on September 23, 1997 of 66.4 m^3/s (largest of the study period) was assumed to provide sufficient shear stress to entrain the largest blocks.

Inspection of the Goodwin Creek site following the September 23, 1997 event disclosed that the largest EH blocks were not entrained. Two reasons for this are proposed. Firstly, the shear stress generated from the flow was not great enough to entrain

Table 3
Failed bank material critical shear stress values using Wiberg and Smith (1987) for the most common bank-toe scenarios (modified from Simon and Darby, 1997b)

Failed bank-material deposition scenario	D_{max} (mm)	D_{max}/k_s	Block density (ρ_s) (kg/m^3)	Corrected shields stress (τ_{cb}^*)	Critical shear stress (τ_c) (N/m^2)
EH on gravel-toe material	420	3.64	1950	0.012	45.2
LH on gravel-toe material	215	1.86	1850	0.019	34.1
LH on failed EH substrate	215	0.39	1850	0.102	183
Gravel-toe material	66	0.57	1740	0.068	32.6

Note: EH = early Holocene, LH = late Holocene.

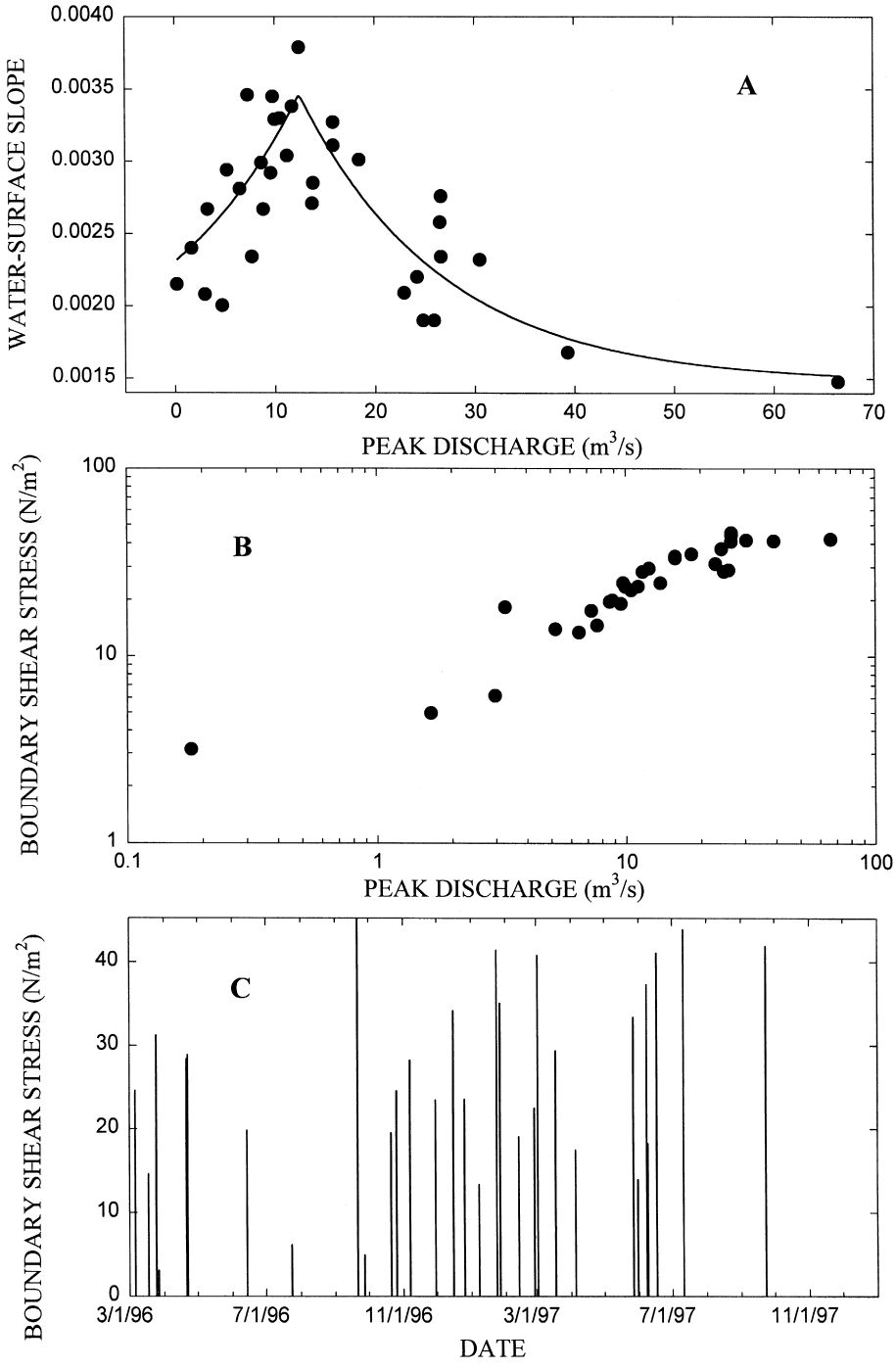

Fig. 9. Hydraulic properties of peak flows measured at Goodwin Creek showing peak in water-surface slopes at about 12 m^3/s (A), effect on boundary shear stress with increasing discharge (B) and calculated boundary shear stresses during the study period (C).

the largest clasts regardless of any additional forces that would result in greater block resistance. With increasing discharge, flows crest a sand–gravel bar at flows above about 12 m^3/s (Fig. 6). As flow continues to increase and the bar becomes covered, flow resistance increases due to herbaceous and woody vegetation on the bar, and because of the sudden increase in the size of the wetted perimeter. Additionally, the rate of increase of flow depth with discharge decreases greatly as the flow spreads out across the bar. The result is that water-surface slopes decrease for flows greater than about 12 m^3/s (Fig. 9A). The effect of decreasing slope with increasing discharge on boundary shear stress can be seen in Fig. 9B. Thus, the flow of September 23, 1997, although twice as deep as previous peak flows with τ equal to 30–40 N/m^2, only attains a shear stress of 42 N/m^2, insufficient to entrain the largest EH blocks. Boundary shear stresses for the period of study are shown in Fig. 9C.

Secondly, although the Shields-type approach used here appears to work reasonably well in predicting entrainment of failed cohesive materials from the bank toe, the approach requires refinement for differentiating between in situ and failed materials, block sizes and shapes at the time of incipient motion, and particularly, to account for the effects of any geotechnical properties which are not accounted for in a Shields-type approach. One such property is the apparent cohesion between a failed cohesive block and the substrate upon which it has been deposited. The potential effect of matric suction on increasing the fluid stress required to entrain a block was tested by measuring ψ at the block-substrate interface. Boundary shear stress values were calculated from the field data.

Typical ψ values at the block-substrate interface during the summer of 1997 are in the order of 5–11 kPa in the region within 0.5 m of the water surface. An average ψ value of 8 kPa can be considered as representative. Assuming a $\phi^b = 17.5°$ results in a cohesion due to suction of 2.5 kPa, a sufficient increment in strength to resist entrainment by the peak flow of 42 N/m^2. Slight decreases in matric suction were observed immediately following a flow event which submerged the blocks on August 19, 1997, but none was significant enough to cause a complete loss of matric suction or to generate positive pore-water pressures at the interface. The low permeability of the materials relative to the short time the blocks are submerged suggests that negative pore-water pressures can be maintained at the base of the blocks during stormflow. This finding helps to explain why the Shields-type approach may not be completely successful in predicting entrainment during the dry summer months.

The fact that shear stresses at high flows are not commensurate with increases in discharge has important implications regarding the effectiveness of high flows in meander extension and elongation in incised channels. Incised channels containing alternate bars and incipient meanders are often aggradational (Simon, 1989a) and have an asymetrical shape with the thalweg on the opposite the high steep bank. Increases in shear stress with increasing discharge, therefore, will characteristically take the form shown in Fig. 9B. This type of relation between discharge and shear stress in incised channels with developing meanders helps to explain why entrainment of bank-toe material by high flows is as effective as entrainment capabilities of much lower flows (Fig. 9B). Entrainment of the largest blocks can occur with time as the largest blocks are reduced in size by raindrop impact, erosion by fluid shear and drag, and by dessication. This allows for fluvial entrainment by relatively small frequent flows. Consequently, it appears that meander extension and elongation can be defined as a sequence of the following processes which operate most effectively at low and moderate flows: bar growth, flow deflection and bank-toe erosion on the opposite bank, bank failure and erosion of failed debris.

6. Conclusions

The interaction of gravitational forces working on in situ bank material with hydraulic forces acting at the bank toe and channel bed determine rates and styles of bank erosion and, therefore, bank morphology. Hydraulic forces exerted by flowing water on in situ bank-toe material and failed cohesive material at the bank toe are often sufficient to entrain materials and to maintain steep low-bank profiles. Seepage forces exerted on in situ bank material by groundwater, downward infiltration of rainwater and lateral

seepage of streamflow are critical in determining bank strength. The data from Goodwin Creek clearly shows the temporal variability of seepage forces and the lag time inherent in reductions in shear strength due to losses of matric suction and generation of positive pore-water pressures. The relation between shear strength and matric suction, defined by the angle ϕ^b was determined from in situ field measurements of apparent cohesion at various values of matric suction, leading to evaluation of the true value of effective cohesion (2.7 kPa). Local extremum of apparent cohesion were also found in the moisture-content domain close to saturation due to increases in ϕ^b as matric-suction values approach 0.0.

Seepage forces (matric suction) have also been shown to increase the resistance of failed cohesive blocks to entrainment by hydraulic forces. A stable bank is transformed into an unstable bank during periods of prolonged rainfall through:

1. increase in soil unit weight,
2. decrease or complete loss of matric suction, and, therefore, apparent cohesion,
3. generation of positive pore-water pressures, and, therefore loss of frictional strength,
4. entrainment of in situ and failed material at the bank toe, and
5. loss of confining pressure during recession of stormflow hydrographs.

Rapid-drawdown conditions formed from persistent rainfall and vertical seepage, combined with the loss of confining pressure during stormflow recession represents the dominant bank-hydrology condition for mass failure. This has occurred predominantly during the winter months at the research site studied. A similar storm, occurring during the summer months generally is not able to destabilize the channel banks because of high antecedent values of matric suction. It is not the largest storms and greatest floods that induce bank failures, but prolonged wet periods, which weaken in situ bank materials resulting in mass failure. Thus, even relatively small frequent flows during the winter have the ability to erode failed bank materials, maintain oversteepened, unstable bank surfaces and promote prolonged periods of bank retreat, channel migration, and high yields of fine-grained sediment. About 2 m of bank retreat occurred at the site over the study period.

The bank-stability algorithm presented here has been used to model the timing and conditions leading to mass failure. The algorithm utilizes time–series data in a dynamic framework to incorporate the effects of matric suction for the portion of the failure plane in the unsaturated zone, confining pressure, positive pore-water pressure, varying soil unit weight and layering within the banks. Geotechnical data used for input into the algorithm were obtained in situ. Continuous surface-water stage and matric-suction data were used to test the algorithm against observed failures. Results show that the bank-stability algorithm (Eq. (11)) was able to predict the timing and conditions of mass failure for a layered cohesive streambank.

Acknowledgements

The following individuals are greatly appreciated for their assistance in this study. Students from the Department of Geography, University of Nottingham: Anna Wood for photographic analysis of particle-size distributions of bank-toe material, John Bromley for collection of matric-suction data at the interface between failed cohesive blocks and in situ bank-toe materials; from the USDA, Agricultural Research Service, National Sedimentation Laboratory, Brain Bell and Mark Griffith are recognized for collection of in situ shear strength data and for weekly downloading of tensiometric data. The authors would also like to thank the Earth Sciences Research Group at the Universita degli Studi di Firenze, Italy.

References

Bagnold, R.A., 1953. Experiments on a gravity free dispersion of large solid spheres in a Newtonian fluid under shear. Proc. R. Soc. London, Ser. A 255, 49–63.

Bagnold, R.A., 1966. An approach to the sediment transport problem from general physics. U.S. Geol. Surv. Prof. Pap. 422-I, 1–37.

Bradford, Piest, 1980. Erosional development of valley-bottom gullies in the upper midwestern United States. In: Coates, D.R., Vitek, J.D. (Eds.), Thresholds in Geomorphology. George, Allen & Unwin Publishers, London, pp. 75–101.

Carson, M.A., Kirkby, M.T., 1972. Hillslope Form and Process. Cambridge Univ. Press, London, 475 pp.

Casagli, N., 1994. Determinazione del fattore di sicurezza per scivolamenti planari nelle sponde fluviali. Studi Geol. Appl. Geol. Ambiente 30, Dipartimento Scienze della Terra, Universita degli Studi di Firenze.

Casagli, N., Curini, A., Gargini, A., Rinaldi, M., Simon, A., 1997. Effects of pore pressure on the stability of streambanks: preliminary results from the Sieve River, Italy. In: Wang, S.S.Y., Langendoen, E.J., Shields, F.D. Jr. (Eds.), Management of Landscapes Disturbed by Channel Incision. pp. 243–248.

Casagli, N., Curini, A., Gargini, A., Rinaldi, M. 1999. Pore water pressure and streambank stability: results from a monitoring site on the Sieve River, Italy.

Curini, A., 1998. Analisi dei processi di erosione di sponda nei corsi d'acqua, Universita degli Studi di Firenze, Dipartimento di Scienze della Terra, 147, unpublished thesis.

Darby, S.E., 1994. A physically based numerical model of river channel widening, PhD thesis, University of Nottingham, UK, 276 pp.

Francis, J.R.D., 1973. Experiments on the motion of solitary grains along the bed of a water stream. Proc. R. Soc. London, Ser. A 332, 443–471.

Fredlund, D.G., 1986. Slope-stability analysis incorporating the effect of soil suction. In: Anderson, M.G., Richards, K.S. (Eds.), Slope Stability. Wiley, Chichester, pp. 113–145.

Fredlund, D.G., Morgenstern, N.R., Widger, R.A., 1978. The shear strength of unsaturated soils. Can. Geotech. J. 15, 313–321.

Fredlund, D.G., Rahardjo, H., 1991. Use of linear and nonlinear shear strength versus matric suction relations in slope stability analyses. In: Bell, D.H. (Ed.), Landslides. Balkema, Rotterdam, pp. 531–537.

Fredlund, D.G., Rahardjo, H., 1993. Soil Mechanics of Unsaturated Soils. Wiley, New York, p. 517.

Fredlund, D.G., Rahardjo, H., Gan, J.K.M., 1987. Nonlinearity of strength envelope for unsaturated soils. Proc. 6th Int. Conf. Expansive Soils (New Delhi, India) 1, 49–54.

Gan, J.K.M., Fredlund, D.G., 1988. Multistage direct shear testing on unsaturated soils. ASTM Geotech. Test. J. 11 (2), 132–138.

Grissinger, E.H., Murphey, J.B., 1983. Present channel stability and late Quaternary valley deposits in northern Mississippi. Spec. Publ. Int. Assoc. Sedimentol. 6, 241–250.

Grissinger, E.H., Murphey, J.B., 1989. Bank stability of Goodwin Creek channel, northern Mississippi, USA. Proceedings, Fourth International Symposium on River Sedimentation, Beijing, China. pp. 59–66.

Grissinger, E.H., Murphey, J.B., Little, W.C., 1981. Problems with Eocene stratigraphy in Panola County, northern Mississippi. Southeast. Geol. 22 (1), 19–28.

Lane, E.W., 1953. Progress report on studies on the design of stable channels of the Bureau of Reclamation. Proc. Am. Soc. Civ. Eng. 79, 246–261.

Lawler, D.M., 1993. The measurement of river bank erosion and lateral channel change: a review. Earth Surf. Processes Landforms 18, 777–821.

Little, W.C., 1982. Mass bank failure analysis of selected Yazoo Basin streams. Trans., Am. Soc. Agric. Eng. 25, 1321–1328.

Lohnes, R.L., 1991. A method for estimating land loss associated with stream channel degradation. Eng. Geol. 31, 115–130.

Lohnes, R.A., Handy, R.L., 1968. Slope angles in friable loess. J. Geol. 76 (3), 247–258.

Luttenegger, J.A., Hallberg, B.R., 1981. Borehole shear test in geotechnical investigations. ASTM Spec. Publ. 740, 566–578.

Millar, R.G., Quick, M.C., 1993. Effect of bank stability on geometry of gravel rivers. J. Hydraul. Eng. 119, 1343–1363.

Murphey, J.B., Grissinger, E.H., 1985. Channel cross-section changes in Mississippi's Goodwin Creek. J. Soil Water Conserv. 40 (1), 148–153.

Osman, A.M., Thorne, C.R., 1988. Riverbank stability analysis: I. Theory. J. Hydraul. Eng. 114 (2), 134–150.

Rinaldi, M., 1994. Dinamica di un alveo fluviale antropizzato: Il Fiume Sieve (Toscana). Dottorato di Ricera in Geologia Applicata, Geomorfologia e Idrogeologia, Universita degle Studi di Perugia, Firenze e Camerino, VII Ciclo 1991–1994, unpublished.

Schumm, S.A., Lichty, R., 1963. Channel widening and flood plain construction along the Cimarron River in south-western Kansas. U.S. Geol. Surv. Prof. Pap. 352D, 71–88.

Simon, A., 1989a. A model of channel response in disturbed alluvial channels. Earth Surf. Processes Landforms 14, 11–26.

Simon, A., 1989b. Shear-strength determination and stream-bank instability in loess-derived alluvium, West Tennessee, USA. In: DeMulder, E.J., Hageman, B.P. (Eds.), Applied Quaternary Research. A.A. Balkema Publishers, Rotterdam, pp. 129–146.

Simon, A., 1992. Energy, time, and channel evolution in catastrophically disturbed fluvial systems. In: Phillips, J.D., Renwick, W.H. (Eds.), Geomorphic Systems: Geomorphology vol. 5 pp. 345–372.

Simon, A., Curini, A., 1998. Pore pressure and bank stability: the influence of matric suction. In: Abt, S. (Ed.), Hydraulic Engineering '98. ASCE, Reston, pp. 358–363.

Simon, A., Darby, S.E., 1997a. Process-form interactions in unstable sand-bed river channels: a numerical modeling approach. Geomorphology 21, 85–106.

Simon, A., Darby, S.E., 1997b. Bank-erosion processes in two incised meander bends: Goodwin Creek, Mississippi. In: Wang, S.S.Y., Langendoen, E.J., Shields, F.D. Jr. (Eds.), Management of Landscapes Disturbed by Channel Incision. pp. 256–261.

Simon, A., Hupp, C.R., 1987. Geomorphic and vegetative recovery processes along modified Tennessee streams: an interdiscilpinary approach to disturbed fluvial systems. IAHS Spec. Publ. 167, 251–262.

Simon, A., Rinaldi, M., Hadish, G., 1996. Channel evolution in the loess area of the midwestern United States. Proceedings, Sixth Federal Interagency Sedimentation Conference, Las Vegas, March 10–14. pp. III-86–III-93.

Simon, A., Wolfe, W.J., Molinas, A., 1991. Mass wasting algorithms in an alluvial channel model. Proc. 5th Fed. Inter-agency Sediment. Conf., Las Vegas, Nevada 2, 8-22–8-29.

Terzaghi, K., Peck, R.B., 1948. Soil Mechanics and Engineering Practice. Wiley, New York, 566 pp.

Thorne, C.R., 1982. Processes and mechanisms of river bank erosion. In: Hey, R.D., Bathurst, J.C., Thorne, C.R. (Eds.), Gravel-Bed Rivers. Wiley, Chichester, England, pp. 227–271.

Thorne, C.R., 1990. Effects of vegetation on riverbank erosion and stability. In: Thornes, J.B. (Ed.), Vegetation and Erosion. Wiley, Chichester, England, pp. 125–144.

Thorne, C.R., 1978. Processes of bank erosion in river channels, University of East Anglia, UK, unpublished PhD thesis.

Thorne, C.R., Murphey, J.B., Little, W.C., 1981. Stream channel stability, Appendix D, Bank Stability and Bank Material Properties in the Bluffline Streams of Northwest Mississippi. U.S. Department of Agriculture Sedimentation Laboratory, Oxford, MS, 257 pp.

Wiberg, P.L., Smith, J.D., 1987. Calculations of the critical shear stress for motion of uniform and heterogeneous sediments. Water Resour. Res. 23, 1471–1480.